

# **A TSUNAMI FORECAST MODEL FOR ARECIBO, PR**

Diego Arcas

# CONTENTS

<b>Foreword .....</b>	<b>3</b>
<b>Abstract .....</b>	<b>3</b>
<b>1.0 Background and Objectives.....</b>	<b>4</b>
<b>2.0 Forecast Methodology .....</b>	<b>5</b>
<b>3.0 Model Development .....</b>	<b>5</b>
3.1 Forecast Area.....	6
3.2 Historical Events and Data .....	6
3.3 Model Setup .....	6
<b>4.0 Results and Discussion .....</b>	<b>8</b>
4.1 Model Validation.....	9
4.2 Model Stability Testing using Synthetic Scenarios.....	9
<b>5.0 Summary and Conclusion .....</b>	<b>10</b>
<b>6.0 Acknowledgments .....</b>	<b>10</b>
<b>7.0 References .....</b>	<b>11</b>
<b>Appendix A .....</b>	<b>13</b>
<b>Appendix B – Propagation Database Unit Sources.....</b>	<b>14</b>
<b>Appendix C .....</b>	<b>15</b>
<b>Appendix D .....</b>	<b>15</b>
<b>Appendix E.....</b>	<b>15</b>

## **Foreword**

Tsunamis have been recognized as a potential hazard to United States coastal communities since the mid-twentieth century, when multiple destructive tsunamis caused damage to the states of Hawaii, Alaska, California, Oregon, and Washington. In response to these events, the United States, under the auspices of the National Oceanic and Atmospheric Administration (NOAA), established the Pacific and Alaska Tsunami Warning Centers, dedicated to protecting United States interests from the threat posed by tsunamis. NOAA also created a tsunami research program at the Pacific Marine Environmental Laboratory (PMEL) to develop improved warning products.

The scale of destruction and unprecedented loss of life following the December 2004 Sumatra tsunami served as the catalyst to refocus efforts in the United States on reducing tsunami vulnerability of coastal communities, and on 20 December 2006, the United States Congress passed the “Tsunami Warning and Education Act” under which education and warning activities were thereafter specified and mandated. A “tsunami forecasting capability based on models and measurements, including tsunami inundation models and maps.” is a central component for the protection of United States coastlines from the threat posed by tsunamis. The forecasting capability for each community described in the PMEL Tsunami Forecast Series is the result of collaboration between the National Oceanic and Atmospheric Administration office of Oceanic and Atmospheric Research, National Weather Service, National Ocean Service, National Environmental Satellite Data and Information Service, the University of Washington’s Joint Institute for the Study of the Atmosphere and Ocean, National Science Foundation, and United States Geological Survey.

## **Abstract**

This study documents the development of a tsunami forecast model for Arecibo, Puerto Rico. The town of Arecibo is located on the Northern coast of the island of Puerto Rico in the Atlantic Ocean. It is, particularly exposed to tsunamis originating in the Puerto Rico trench approximately 100 km north of the island. The Puerto Rico Trench separates the North American and Caribbean plates and extends for approximately 1750 km with a width of almost 100 km. Its deepest (Milwaukee Point) is the deepest point outside of the Pacific Ocean.

Since there is no quantitative information about large historical tsunami events for the island of Puerto Rico, it is not possible to use such events for validation of the inundation forecast model for Arecibo. Accuracy of the results is addressed in this study by comparing the solution obtained using the forecast model and that obtained with a higher resolution model for 6 synthetic mega-tsunami scenarios originating in different regions of the Caribbean and Atlantic Ocean. In addition to the mega-tsunami scenarios a more probable  $M_w=7.5$  scenario is also simulated as well as a micro-tsunami triggered by a seismic event in the South Sandwich Islands, located in the South Atlantic.

Results from this study confirm that the Puerto Rico Trench poses the largest tsunami

hazard to the town of Arecibo.

## **1.0 Background and Objectives**

The Pacific Marine Environmental Laboratory (PMEL) of the National Oceanic and Atmospheric Administration (NOAA) Center for Tsunami Research (NCTR) has developed a tsunami forecasting capability for operational use by NOAA's two Tsunami Warning Centers located in Hawaii and Alaska (Titov et al. 2005). The system is designed to efficiently provide basin-wide warning of approaching tsunami waves. The system termed Short-term Inundation Forecast of Tsunamis (SIFT) combines real-time tsunami event data with numerical models to produce estimates of tsunami wave arrival times and amplitudes at a coastal community of interest. The SIFT system integrates several key components: deep-ocean, real-time observations of tsunamis, a basin-wide pre-computed propagation database of water level and flow velocities based on potential seismic unit sources, an inversion algorithm to refine the tsunami source based on deep-ocean observations during an event, and optimized tsunami forecast models.

The objective of the present work is to construct a tsunami inundation model for Arecibo, Puerto Rico that can be used by the Tsunami Warning Centers to assess, in real time, the local impact of a tsunami generated anywhere in the Caribbean or Atlantic Ocean.

The most relevant bathymetric feature offshore of Arecibo is the Puerto Rico Trench. The trench is the result of the Caribbean and North American plates sliding past each other and is the deepest point in the Atlantic Ocean. It has the potential for triggering large tsunami events, having generated earthquakes with magnitude larger than 8.0 in the past, such as the 1787 event. At a more local scale, the other relevant bathymetric feature, off-shore of Arecibo is the presence of the Arecibo Canyon, a submarine valley that could potentially behave as a tsunami wave-guide.

This report details the development of a high-resolution tsunami forecast model for Arecibo, PR including development of the bathymetric grids, model validation and stability testing with a set of synthetic mega-tsunami events (Mw 9.3). Inundation results from such artificial events are presented in later sections.

## **2.0 Forecast Methodology**

A high-resolution inundation model was used as the basis for the operational forecast model to provide an estimate of wave arrival time, height, and inundation immediately following tsunami generation. Tsunami forecast models are run in real time while the tsunami in question is propagating across the open ocean. These models are designed and tested to perform under very stringent time constraints given that time is generally the single limiting factor in saving lives and property. The goal is to maximize the amount of time that an at-risk community has to react to a tsunami threat by providing accurate information quickly. To this end, the tsunami propagation solution in deep water is pre-computed in the linear wave regime and used to force the inundation forecast models during the last stage of tsunami propagation and runup.

The tsunami forecast model, based on the Method of Splitting Tsunami (MOST),

emerges as the solution in the SIFT system by modeling real-time tsunamis in minutes. SIFT employs high-resolution grids constructed by the National Geophysical Data Center or, in limited instances, internally. Each forecast model consists of three telescoped grids with increasing spatial and temporal resolution for simulation of wave inundation onto dry land. The forecast model utilizes the most recent bathymetry and topography available to reproduce the correct wave dynamics during the inundation computation. Forecast models are constructed for at-risk populous coastal communities in the Pacific and Atlantic Oceans. Previous and present development of forecast models in the Pacific (Titov *et al.*, 2005; Titov, 2009; Tang *et al.*, 2009; Wei *et al.*, 2008) have validated the accuracy and efficiency of the forecast models currently implemented in the SIFT system for real-time tsunami forecast. The model system is also a valuable tool in hind-cast research. Tang *et al.* (2009) provides forecast methodology details.

### 3.0 Model Development

Modeling of coastal communities is accomplished by development of a set of three nested grids that telescope down from a large spatial extent to a grid that finely defines the bathymetric and topographic features of the community under study. The original bathymetric and topographic grid data used in the development of the Arecibo model were provided by the National Geophysical Data Center (NGDC) under PMEL contract. Details of data gathering and grid construction techniques used by NGDC in the generation of the original grid are provided by Taylor *et al.* For each community, data are compiled from a variety of sources to produce a digital elevation model referenced to Mean High Water in the vertical and to the World Geodetic System 1984 in the horizontal (<http://ngdc.noaa.gov/mgg/inundation/tsunami/inundation.html>). From these digital elevation models, a set of three high-resolution reference models are constructed which are then “optimized” to run in an operationally specified period of time.

### 3.1 Forecast Area

The city of Arecibo is located on the northern coast of the island of Puerto Rico approximately 70 km east of the capital city of San Juan. Arecibo’s population is estimated at 95,816 according the U.S. Census (2011). It is nestled between the rivers Grande de Arecibo and Tanamá.

Arecibo is a medium size agricultural community, according to the Fundación Puertorriqueña de las Humanidades: “The fertility of the land in Arecibo favored the development of agriculture, and the principal crop in the first half of the 20<sup>th</sup> century was sugar cane. Pineapple and other fruits were also planted. Arecibo also had a wealth of livestock ranches. The Arecibo River is known for its freshwater fish. Other sources of income for the municipality are the operation of various manufacturing factories in areas such as distilling and the production of paper, clothing, and chemical products.” (Fundación Puertorriqueña de las Humanidades,

<http://www.encyclopediapr.org/ing/article.cfm?ref=09022301&page=2>).

Among the geographic features of Arecibo relevant to the evaluation of tsunami impact,

are: The presence of a large coastal lagoon that extends for over 15 km to the East of Arecibo (see Figure 1), the valley carved by the Grande de Arecibo river, which defines the most likely inundation area, and the presence of several islets such as Punta Caracoles and Los Negritos which may pose some challenges to tsunami numerical simulations.

Puerto Rico is located at the northeastern corner of the Caribbean plates, on the boundary between the Caribbean and the North American plate. These two plates slide past each other in an oblique direction at a remarkably high rate of 2 cm/year for geological standards (USGS Science for a Changing World, Earthquake and Tsunamis in PR and the U.S. VI) as sketched in Figure 2. This generates a significant amount of seismicity north and south of the island. Clear evidence of this is that USGS research indicates equal probability for damaging ground motion for the town of Mayaguez in western Puerto Rico as for Seattle, WA (USGS Science for a Changing World, Earthquake and Tsunamis in PR and the U.S. VI). To the north of the island most of the tsunami-generating seismic events occur in the Puerto Rico Trench whereas the Muertos Trough is the generating area for tsunamis impacting the island from the south. Arecibo is located on the northern coast of the island of Puerto Rico, and it is, particularly vulnerable to tsunamis generated in the Puerto Rico Trench. However, far-field tsunamis originating in the Marqués de Pombal fault, offshore of Portugal have also been recorded on the island, such is the case of the 1755 Lisbon tsunami event. Table 1 contains a list of the most significant historical near-field seismic events in the island of Puerto Rico.

### **3.2 Historical Events and Data**

A NOS (9757809) operated tide gauge was deployed on the Arecibo pier ( $18.48052^{\circ}$  N,  $66.70236^{\circ}$  W) on March 5th 2007. The gauge is located by the breakwater on the northeastern corner of Arecibo Beach, extending southwest from the Arecibo lighthouse. The lower right panel of Figure 3 shows the location of the tide gauge within the inundation grid (grid C) of the forecast model. As mentioned earlier, Table 1 shows a list of the most significant recent near-field events impacting the island of Puerto Rico, however no tide gauge data of recent tsunamis at this location were found. So no tide gauge data could be used in the historical validation of this forecast model. Therefore the validation of the forecast model was based on comparison of high-resolution model results with forecast model results.

### **3.3 Model Setup**

Setup of the computational grids for the Method of Splitting Tsunami code (MOST) (Titov, 1998) requires a total of 3 nested grids for which the outer grid A has the lowest spatial resolution, but covers the largest area, and the inner grid C has the highest spatial resolution, but covers a reduced geographical area. The code makes use of an additional intermediate grid B with medium resolution and spatial coverage. Each interior grid area is completely enclosed in the area covered by the next exterior grid, and inundation is computed only in the most interior grid (Grid C). The purpose of the set of three nested

grids is to ensure that as the tsunami wavelength shrinks when it travels from deep to shallow waters, the model maintains an approximately constant number of grid nodes per wavelength. This set of 3 nested grids is forced by a pre-computed solution on an ocean wide grid at lower resolution (4 arc min x 4 arc min). The resolution of the this propagation grid was selected to mimic the effect of physical dispersion by manipulating numerical dispersion in the model (Burwell *et al.* 2007) .

During the development of an operational forecast model, a higher resolution set of grids referred to as the reference model is generated first. The purpose of the reference model is to evaluate grid convergence between a high resolution model and the forecast model, ensuring that the solution obtained with the lower resolution forecast model is consistent with that computed with the high resolution reference model.

Several factors were determining in the design of the Arecibo model grids. One of them is the presence of extensive areas of extremely shallow water around the Caribbean arc. Tsunami waves propagating over these shallow regions will experience a shortening of their wavelength as they approach the island of Puerto Rico. It is important, therefore, to model wave propagation over these areas using a higher resolution grid than that used for the simulations stored in the deep-water propagation database (4 arc min resolution). This is accomplished in the present model by extending the most outer grid of the set of three nested grids (Grid A) towards the east and south of Puerto Rico. The resolution of Grid A in the present model is 47.24 arc sec in the zonal direction and 4 arc sec in the meridional direction, permitting the resolution of much higher frequency waves over shallow regions than the 4 arc min propagation database grid.

In addition, the A-grid used in the current forecast model is identical to that used in other Caribbean region forecast models, such as that for Charlotte Amalie in the U.S. Virgin Islands. This set up has the potential to be advantageous in future configurations of SIFT software, since it will make it possible to compute the A-grid only once and share the computation results with all forecast models located within the geographical extent of the grid, avoiding multiple computations of the same grid for different forecast models.

An additional consideration when designing the Arecibo forecast model grids was the local topography. The area around the town of Arecibo shows some regions of low-lying coastal planes susceptible of being inundated by tsunami waves. The southern boundary of the model's inundation grid (Grid C) was located far enough inland that most of the coastal plane is included in the grid. This configuration will ensure that even in the worst case scenario, tsunami runoff will not exceed the grid boundaries.

The location of a densely populated coastal area mostly to the west of the tide gauge location was also a consideration when determining the location of the western boundary of the grid.

Figure 3 highlights the difference between the reference and the forecast model grids and Figures 4 and 5 show grid coverage area and relative grid position with respect to the community and local bathymetric features, for the reference and forecast models respectively. Table 2 summarizes the parameters and model set up for each set of grids.

## 4.0 Results and Discussion

Typically three types of tests are performed to assess the forecast model convergence, accuracy and robustness characteristics. However, in the case of Arecibo, since no historical data are available, accuracy tests based on historical events could not be performed.

To assess model convergence, results obtained with the reference model were compared with those obtained with the forecast model to confirm consistency of results at least for the leading tsunami waves. This type of test is not, strictly speaking, a grid convergence test in the sense used in computational science, since the solution is compared on grids with varying resolution, coverage and bathymetric information; however, it provides a good estimate of the similarities and discrepancies between the solution of a more accurate, high resolution model of the area and that of a coarser resolution run-time optimized forecast model.

Robustness tests include the simulation of 6 tsunamis generated by Mw 9.3 earthquakes throughout the Caribbean and Atlantic basin, a medium magnitude event (Mw=7.5) and a small magnitude (micro tsunami, Mw=6.2) event. Figure 6 shows the epicenter locations of these artificial events. Forecast model simulations proved to be free of instabilities during 24 hours of simulation for each of these synthetic mega events.

During the development of the present forecast model, it was observed when examining the animations of events with local co-seismic deformation in Arecibo, the presence of a west-travelling wave from the eastern boundary of the coastal lagoon (right edge of grid C) into the lagoon. The cause of this is that the current operational version of MOST modifies the local bathymetry in the case of local seismic deformation, but it does not modify the topography. Grid nodes interior to the coastal lagoon are considered bathymetric nodes (wet points) and experience subsidence during a local event. MOST applies the computed subsidence to these grid nodes, effectively lowering the water level in the lagoon below sea level. On the eastern boundary of the coastal lagoon (eastern edge of Grid C) wave values are interpolated from near-by exterior nodes in Grid B, some of those nodal values correspond to land values with 0 wave elevation, consequently the wave value along the eastern boundary of the lagoon is the average of some neighboring wet points (lagoon wet points in Grid B) and some dry points that fall outside of the lagoon in Grid B, the wet points have subsided below sea level due to the seismic deformation by the same amount as the lagoon wet points in Grid C, but the dry points maintain a wave height value of 0, resulting in a negative average interpolated wave height value to be interpolated into the lagoon boundary. The difference in wave height causes a positive wave to be interpolated into the eastern boundary of the lagoon. The problem was resolved by modifying the MOST code so that no bathymetric co-seismic deformation was applied to the coastal lagoon, however this was a specific fix that worked for the Arecibo forecast model. When the forecast model is executed in SIFT it will run with the operational version of MOST and this left travelling wave will be visible in the lagoon for near-field simulations. This wave was small enough that it did not seem to have a major effect on the overall prediction.

## **4.1 Model Validation**



As there are no recorded historical cases for Arecibo, the validity of the forecast model was therefore assessed by comparing the forecast model solution with that obtained using the high resolution model for 8 synthetic scenarios. Since most of the tested scenarios are  $M_w=9.3$ , this set of tests was also used to establish the stability of the forecast model.

## **4.2 Model Stability Testing using Synthetic Scenarios**

During model stability testing, 8 synthetic tsunamis (earthquake  $M_w$  9.3,  $M_w$  7.5, and  $M_w$  6.2) were simulated using the forecast model. Details of the 8 synthetic events tested can be found in Table 3. Each of the six extreme synthetic mega events is constructed along a 1000 km long and 100 km wide fault plane with uniform slip amount of 25 m along the fault. The output from the code at every time step was visualized and inspected for instabilities. The cause of any instability was corrected and a final set of forecast grids emerged from the process. Most of the forecast model instabilities were associated with deficient resolution to distinguish small bathymetric and topographic features.

Six of the eight synthetic events used as test cases in this study were generated by earthquakes with epicenters located at different points along the Caribbean arc. The micro tsunami event ( $M_w=6.2$ ) was designed to be generated by a far-field earthquake in the South Sandwich Islands. Time series comparison of the results obtained with the high resolution model and with the forecast model show very good agreement, with almost a one to one comparison during the first hour of simulation for all cases as evidenced in Figures 7 through 14. However, any differences between the high resolution and forecast model simulations during the first hour of simulation were reflected in discrepancies in the maximum amplitude of the wave train between both simulations. Some of the simulations such as those for Synthetic Scenarios 4 and 6 show excellent comparison between the two models even 24 hours into the simulation.

Of all six mega tsunami events tested, Synthetic Scenario 2 is the one posing the largest tsunami hazard to Arecibo with predicted wave amplitude of almost 15 m at the Arecibo tide gauge. Not surprisingly, Synthetic Scenario 2 represents a  $M_w=9.3$  tsunami scenario generated in the Puerto Rico Trench, directly offshore of the coast of Arecibo. This is without a doubt the worst case scenario for Arecibo of all cases tested during the present study as evidenced in Figures C1 and C2 in Appendix C. Synthetic Scenario 2 is also the worst case scenario for the eastern seaboard of the United States. However, this scenario was designed merely to test the stability and performance of the forecast model during a very large local event. The credibility of such a scenario as a viable earthquake event at that location has not been taken into consideration, consequently these results should not be interpreted as a tsunami hazard study for the Arecibo or the East coast of the United States, but as numerical exercises to test the computational stability of the forecast model.

Additional cases generating a certain amount of inundation at Arecibo are Synthetic Scenarios 1 and 5, with tsunamis originating along the eastern segment of the Caribbean arc and off of the Caribbean coastline of Honduras, respectively. Figures 15 through 22 show the comparison between the inundation extents and maximum wave amplitudes for all 8 synthetic scenarios computed with the reference and forecast models.

## **5.0 Summary and Conclusion**

A set of tsunami forecast grids has been developed for operational use by the Tsunami Warning Centers in conjunction with the Method of Splitting Tsunami code. Two sets of grids were developed: a high resolution set intended to provide reference values, and a forecast set designed to minimize processor run time and to provide real time tsunami estimates in Arecibo, Puerto Rico.

During model development, some geographical features unique to Arecibo such as the presence of very extensive shallow areas along the Caribbean arc and the presence of a coastal lagoon in the town of Arecibo were taken into consideration during the grid design process, some of these considerations will also affect the efficiency of future versions of the SIFT software, such as the ability to run a single Grid A for all locations in the island of Puerto Rico and the U.S. Virgin Islands.

The standard procedure, followed in the development of other forecast models in the Pacific Ocean, of testing the accuracy of the model with data from historical events and evaluating computed results with observations could not be performed in this case due to the lack of good quantitative data for recent historical tsunami events in the area. Therefore accuracy of the forecast model had to be evaluated in conjunction with its stability by comparing forecasted results of a series of mega-tsunami events with results obtained on a set of higher resolution grids.

Even though the magnitude of the set of synthetic events selected to perform stability tests on the forecast model may not necessarily represent credible seismic scenarios, the directivity of their tsunamis can be interpreted as an indicator of what parts of the Caribbean pose the largest tsunami hazard for Arecibo. In this respect, the results of our simulations show that an event in the Puerto Rico Trench immediately offshore of Arecibo represents the worst case scenario, followed by events from the East and West boundaries of the Caribbean arc.

The design of the forecast model grids to include the shallow water areas along the Caribbean arc with as high resolution as possible and the decision to share Grid A with the forecast model for Charlotte-Amalie, U.S. Virgin Islands had minor impact on processor run time and the forecast model was still capable of simulating 4 hours of tsunami activity in 11.35 minutes of wall clock time on an Intel Xeon E5670 2.3 processor.

## **6.0 Acknowledgments**

This research is funded by the NOAA Center for Tsunami Research (NCTR). The authors would like to thank the modeling group of NCTR for their helpful suggestions and discussions. This publication is partially funded by the Joint Institute for the Study of the Atmosphere and Ocean (JISAO) under NOAA cooperative agreement No. NA17RJ1232, JISAO Contribution No. This is PMEL contribution No.

## 7.0 References

Burwell, D., E. Tolkova, A. Chawala (2007): Diffusion and dispersion characterization of a numerical tsunami model. *Ocean Modelling*, Vol. 19, Issues 1-2, ISSN 1463-5003.

Tang, L., V.V. Titov, and C.D. Chamberlin (2009): Development, testing, and applications of site-specific tsunami inundation models for real-time forecasting. *J. Geophys. Res.*, 114, C12025, doi: 10.1029/2009JC005476.

Titov, V.V., and C.E. Synolakis (1998): Numerical modeling of tidal wave runup. *J. Waterw. Port Coast. Ocean Eng.*, 124(4), 157–171.

Titov, V.V., F.I. González, E.N. Bernard, M.C. Eble, H.O. Mofjeld, J.C. Newman, and A.J. Venturato (2005): Real-time tsunami forecasting: Challenges and solutions. *Nat. Hazards*, 35(1), Special Issue, U.S. National Tsunami Hazard Mitigation Program, 41-58.

Titov, V.V. (2009): Tsunami forecasting. In *The Sea*, Vol. 15, Chapter 12, Harvard University Press, Cambridge, MA, and London, England, 371–400.

Taylor LA et al. Digital Elevation Models for Puerto Rico: Procedures, Data Sources and Analysis. National Geophysical Data Center. June 22 2007.

Wei, Y., E. Bernard, L. Tang, R. Weiss, V. Titov, C. Moore, M. Spillane, M. Hopkins, and U. Kânoğlu (2008): Real-time experimental forecast of the Peruvian tsunami of August 2007 for U.S. coastlines. *Geophys. Res. Lett.*, 35, L04609, doi: 10.1029/2007GL032250.

U.S. Census:

[http://factfinder2.census.gov/faces/tableservices/jsf/pages/productview.xhtml?pid=DEC\\_10\\_DP\\_DPDP1](http://factfinder2.census.gov/faces/tableservices/jsf/pages/productview.xhtml?pid=DEC_10_DP_DPDP1)

USGS Science for a Changing World, Earthquake and Tsunamis in PR and the U.S. VI

<http://maps.google.com/>

## Appendix A

### A1. Reference Model \*.in file for Arecibo

```
0.0001 Minimum amplitude of input offshore wave (m):
1      Input minimum depth for offshore (m)
0.1    Input "dry land" depth for inundation (m)
0.0009 Input friction coefficient (n**2)
1      let a and b run up
300.0  max eta before blow up (m)
.38    Input time step (sec)
114000 Input amount of steps
5      Compute "A" arrays every n-th time step, n=6
2      Compute "B" arrays every n-th time step, n=
80     Input number of steps between snapshots
1      ...Starting from
1      ...Saving grid every n-th node, n=
bathy/Anew20s_1nd_SSL1.9sm.asc1
bathy/GridB_RIM.crr.ssl
bathy/GridC_RIM.crr.ssl.flt.snk3
../SRCS/Arecibo_srcs/
./rsyn01_run2d/
1 1 1 1
1
3 333 155
```

### A2. Forecast Model \*.in file for Arecibo

```
0.0001 Minimum amplitude of input offshore wave (m):
1      Input minimum depth for offshore (m)
0.1    Input "dry land" depth for inundation (m)
0.0009 Input friction coefficient (n**2)
1      let a and b run up
300.0  max eta before blow up (m)
0.7    Input time step (sec)
41300  Input amount of steps
6      Compute "A" arrays every n-th time step, n=6
2      Compute "B" arrays every n-th time step, n=
84     Input number of steps between snapshots
```

```

1      ...Starting from
1      ...Saving grid every n-th node, n=
arecibo_run2d/A5_45s_1nd_SSL1.9.asc
arecibo_run2d/GridB_SIM.crr.ssl2
arecibo_run2d/GridC_SIM.crr.ssl.flt.snk.ssl.9.crp2
./
./
1 1 1 1 NetCDF output for A, B, C, SIFT
1      Timeseries locations:
3 118 78

```

## **Appendix B – Propagation Database Unit Sources**

## **Appendix C**

## List of Figures

**Figure 1:** Aerial view of the Puerto Arecibo showing the beach, the pier and location of the tide gauge to the right of the image, the mouth of the Grade de Arecibo River and population center to the left of the image (Google Maps).

**Figure 2:** Schematic of tectonic motion and location of major bathymetric features in the neighborhood of Puerto Rico (from USGS Science for a Changing World, Earthquake and Tsunamis in PR and the U.S. VI).

**Figure 3:** Comparison between the Reference and Forecast model grids. The location of the Arecibo tide gauge on the south side of the pier is indicated in the lower right panel.

**Figure 4:** Map of the Northeastern Caribbean arc showing the relative position of the reference model grids relative to Arecibo and the island of Puerto Rico.

**Figure 5:** Map of the Northeastern Caribbean arc showing the relative position of the forecast model grids relative to Arecibo and the island of Puerto Rico.

**Figure 6:** Location of the mid-rupture point of the 8 synthetic ( $M_w=9.3$ ) events used in the model robustness tests, showing the relative position of Puerto Rico to the epicenter locations.

**Figure 7:** Comparison at the Arecibo tide gauge of the forecast and reference models for Synthetic Scenario 1.

**Figure 8:** Comparison at the Arecibo tide gauge of the forecast and reference models for Synthetic Scenario 2.

**Figure 9:** Comparison at the Arecibo tide gauge of the forecast and reference models for Synthetic Scenario 3.

**Figure 10:** Comparison at the Arecibo tide gauge of the forecast and reference models for Synthetic Scenario 4.

**Figure 11:** Comparison at the Arecibo tide gauge of the forecast and reference models for Synthetic Scenario 5.

**Figure 12:** Comparison at the Arecibo tide gauge of the forecast and reference models for Synthetic Scenario 6.

**Figure 13:** Comparison at the Arecibo tide gauge of the forecast and reference models for Synthetic Scenario 7.

**Figure 14:** Comparison at the Arecibo tide gauge of the forecast and reference models for Synthetic Scenario 8.

**Figure 15:** Maximum sea surface elevation computed with the reference (left) and forecast (right) models for Synthetic Scenario 1.

**Figure 16:** Maximum sea surface elevation computed with the reference (left) and forecast (right) models for Synthetic Scenario 2.

**Figure 17:** Maximum sea surface elevation computed with the reference (left) and forecast (right) models for Synthetic Scenario 3.

**Figure 18:** Maximum sea surface elevation computed with the reference (left) and forecast (right) models for Synthetic Scenario 4.

**Figure 19:** Maximum sea surface elevation computed with the reference (left) and forecast (right) models for Synthetic Scenario 5.

**Figure 20:** Maximum sea surface elevation computed with the reference (left) and forecast (right) models for Synthetic Scenario 6.

**Figure 21:** Maximum sea surface elevation computed with the reference (left) and forecast (right) models for Synthetic Scenario 7.

**Figure 22:** Maximum sea surface elevation computed with the reference (left) and forecast (right) models for Synthetic Scenario 8.

**Figure C1:** Computed Atlantic-wide maximum sea surface elevation for Synthetic Scenarios 1-4.

**Figure C2:** Computed Atlantic-wide maximum sea surface elevation for Synthetic Scenarios 5-8.

#### List of Tables

- 1 Most significant earthquakes in the Puerto Rico area in the last 3 centuries.
- 2 MOST setup parameters for reference and forecast models for Arecibo.
- 3 Synthetic tsunami sources used in the forecast model stability test for Arecibo showing tide gauge max and min water level elevations.

Earthquake location	Date	Magnitude
Hispaniola	1953	6.9
Mona Canyon	1946	7.5
Hispaniola	1946	8.1
Mona Canyon	1918	7.5
Anegada Trough	1867	7.5
Puerto Rico Trench	1787	8.1



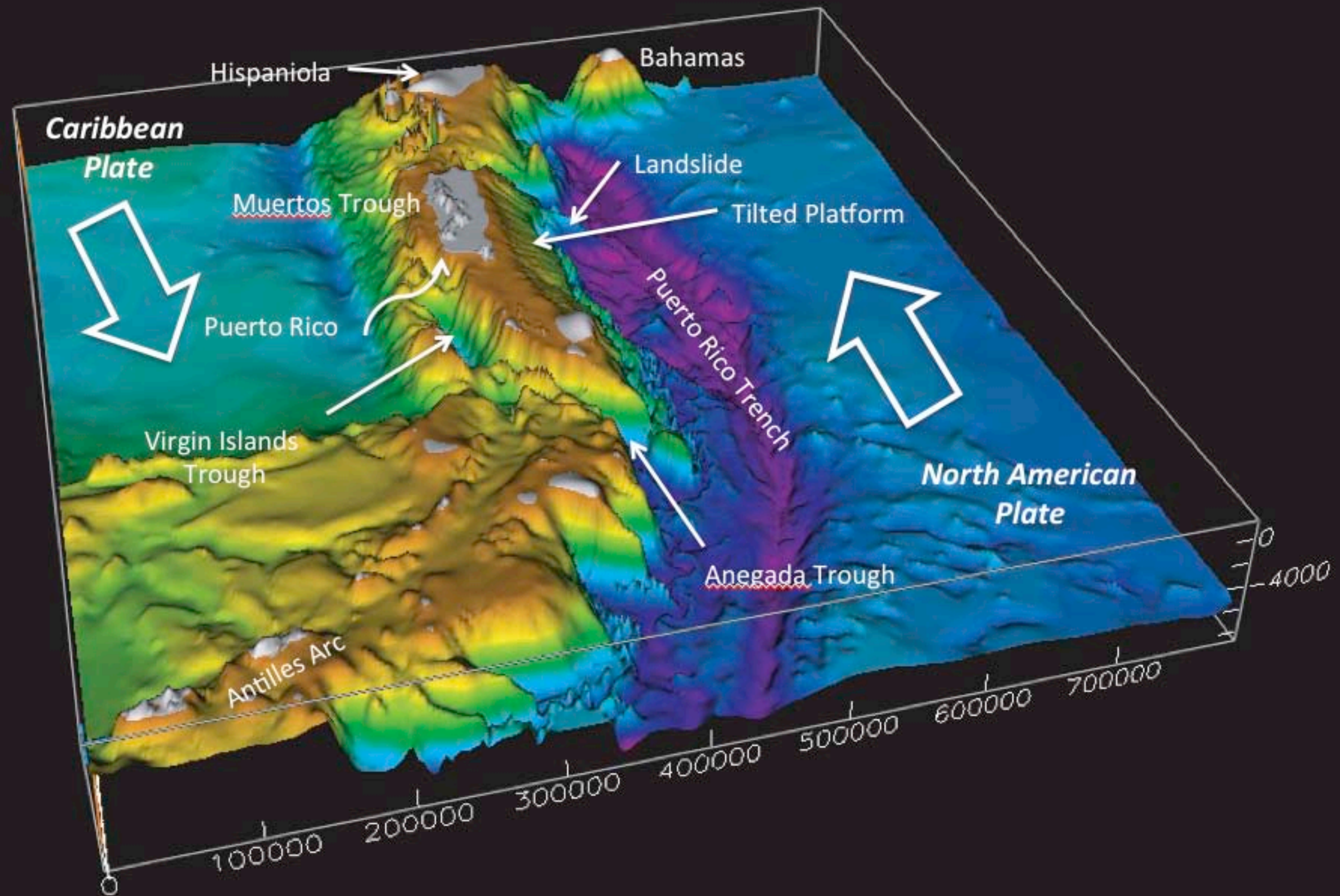
Model Setup	Reference Model			Forecast Model		
	Grid A	Grid B	Grid C	Grid A	Grid B	Grid C
W	W69.90	W66.92	W66.80	W69.00	W66.87	W66.775
E	W60.50	W66.34	W66.63	W61.00	W66.53	W66.281
S	N18.95	N18.70	N18.52	N18.95	N18.60	N18.522
N	N16.05	N18.28	N18.41	N16.50	N18.35	N18.411
$dx$	20.97"	6"	1"	47.24"	6"	2"
$dy$	20"	6"	1"	45"	6"	2"
$nx \times ny$	1614×523	351x251	601×401	610×197	201x153	252×201
$dt$ (sec)	2.3	1.23	1.00	5.2	1.58	0.78
$D_{\min}$	1 m			1 m		
Fric. ( $n^2$ )	0.0009			0.0009		
CPU Time	~ 114.76 min for 4-hour simulation			~ 11.35 min for 4-hour simulation		
Warning Pt.	W66.70144, N18.47912					

SceNo.	Scenario Name	Source Zone	Tsunami Source	$\alpha$ (m)	Max (m)	Min (m)
<b>Mega-tsunami scenario</b>						
1	ATSZ 38-47	Atlantic	A38-A47, A38-A47	25	2.52	-3.38
2	ATSZ 48-57	Atlantic	A48-A57, B48-B57	25	14.3	-5.83
3	ATSZ 58-67	Atlantic	A58-A67, B58-B67	25	0.52	-0.59
4	ATSZ 68-77	Atlantic	A68-A77, B68-B77	25	0.11	-0.09
5	ATSZ 82-91	Atlantic	A82-A91, B82-B91	25	3.17	-3.29
6	SSSZ 1-10	South Sandwich	A1-A10, B1-B10	25	0.14	-0.14
<b>Mw 7.5 Tsunami scenario</b>						
7	ATSZ B52	Atlantic	B52	1	0.10	-0.16
<b>Micro-tsunami scenario (select one)</b>						
8	SSSZ B11	South Sandwich	B11	0.01	<u>0.0002</u>	<u>-0.0003</u>

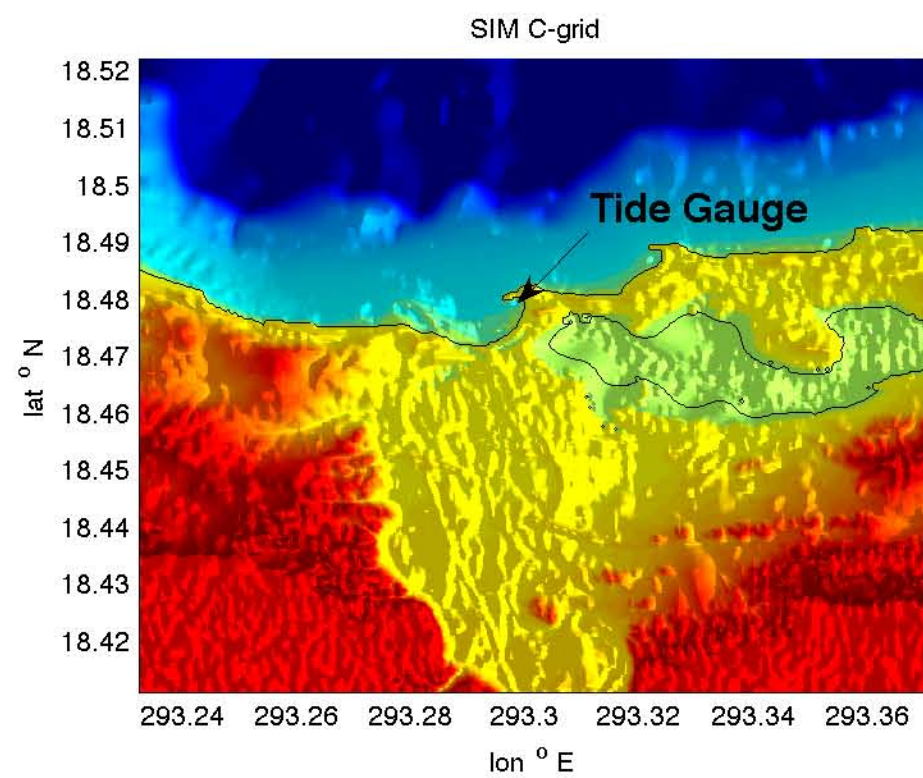
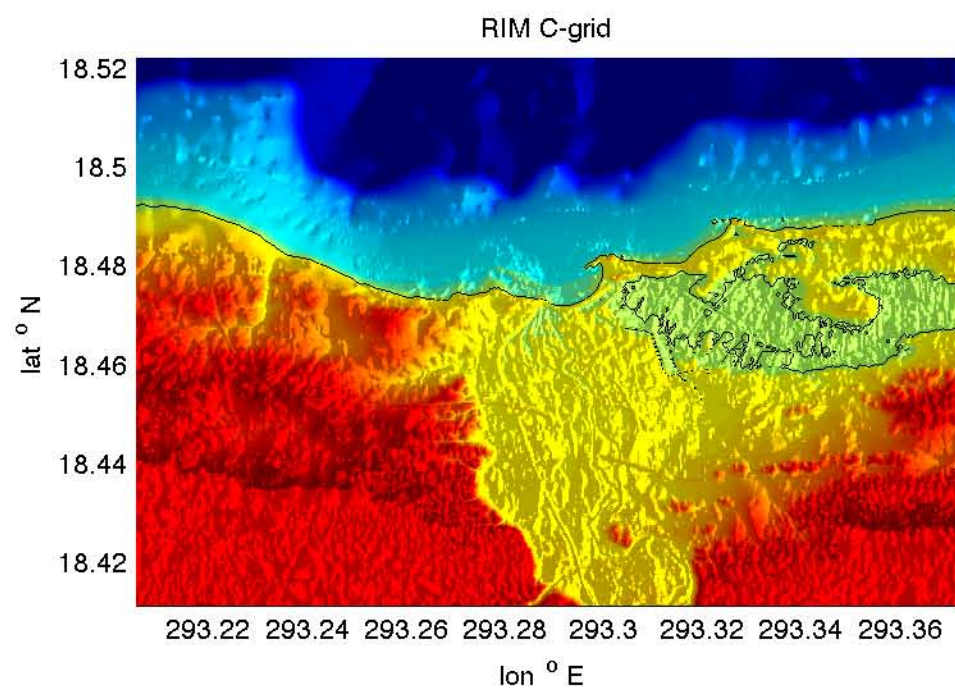
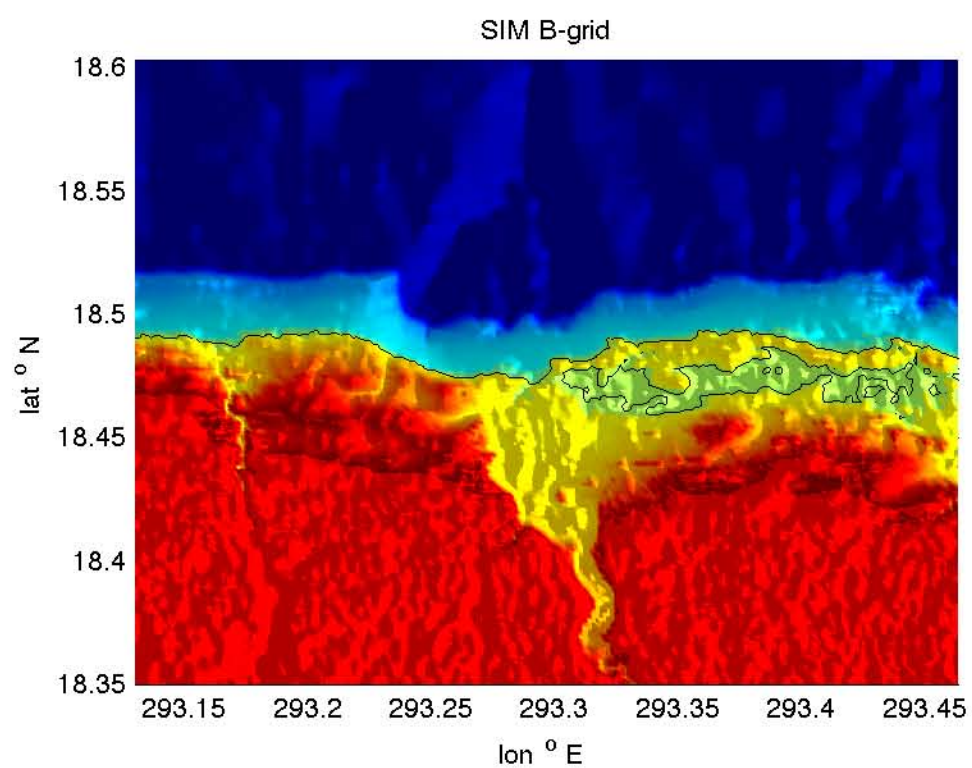
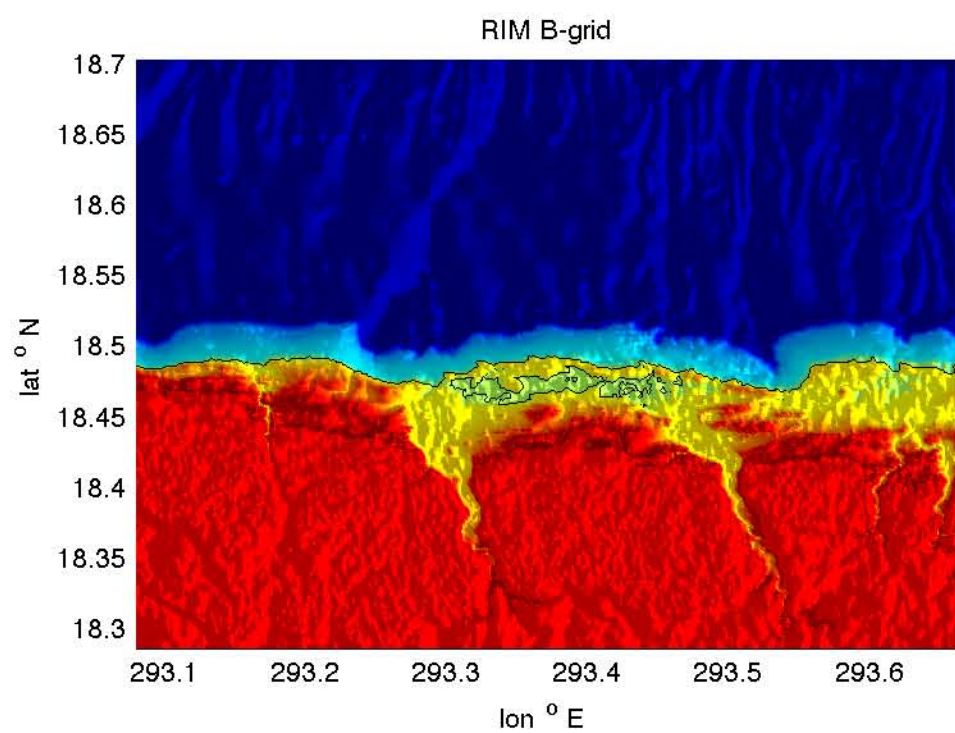
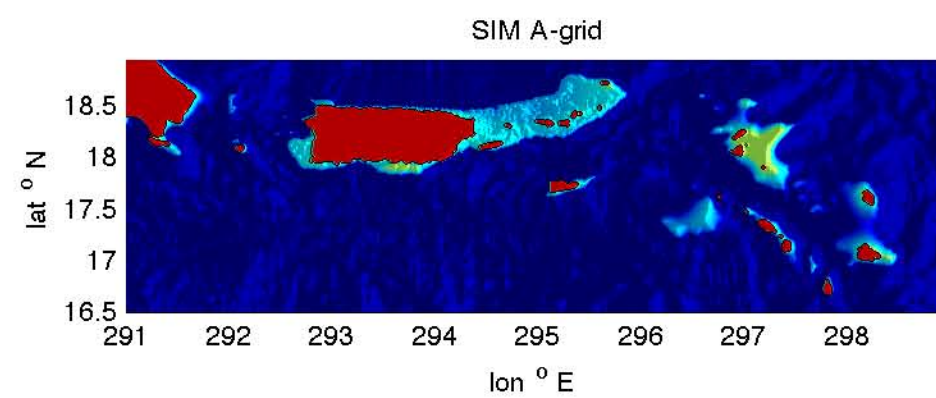
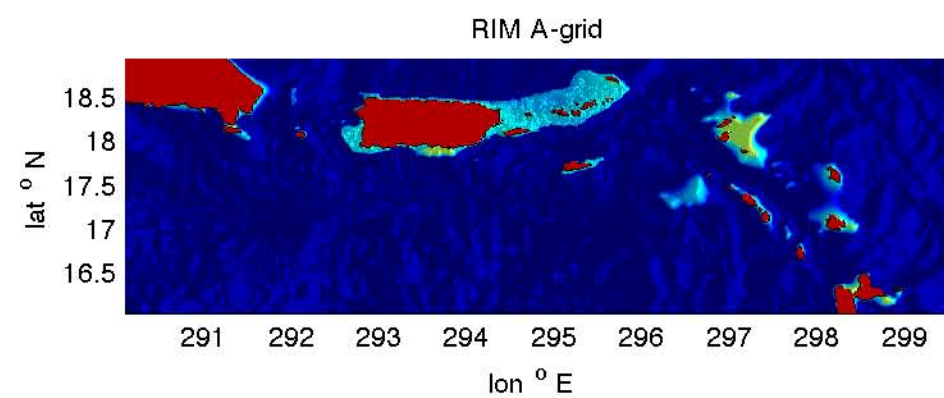






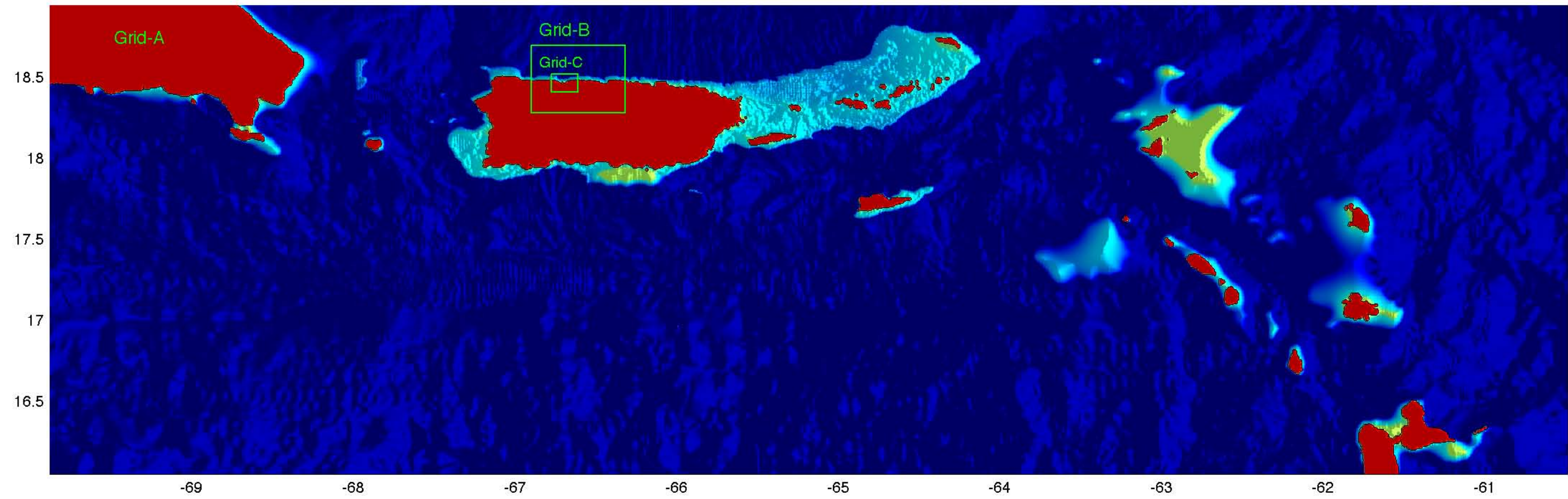




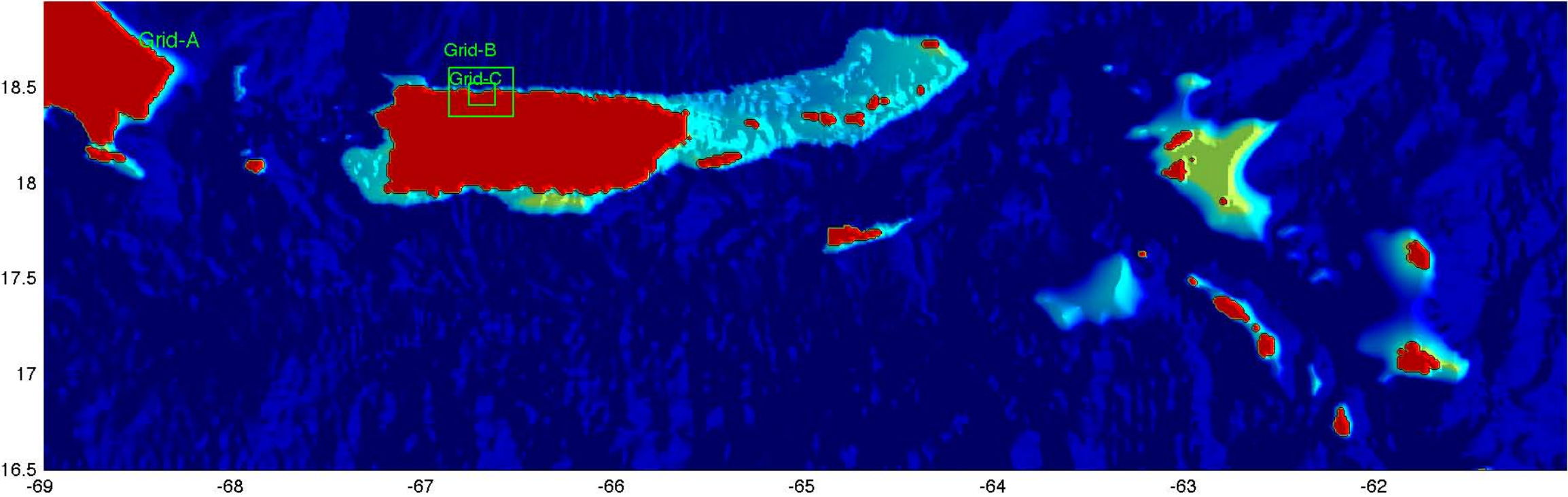


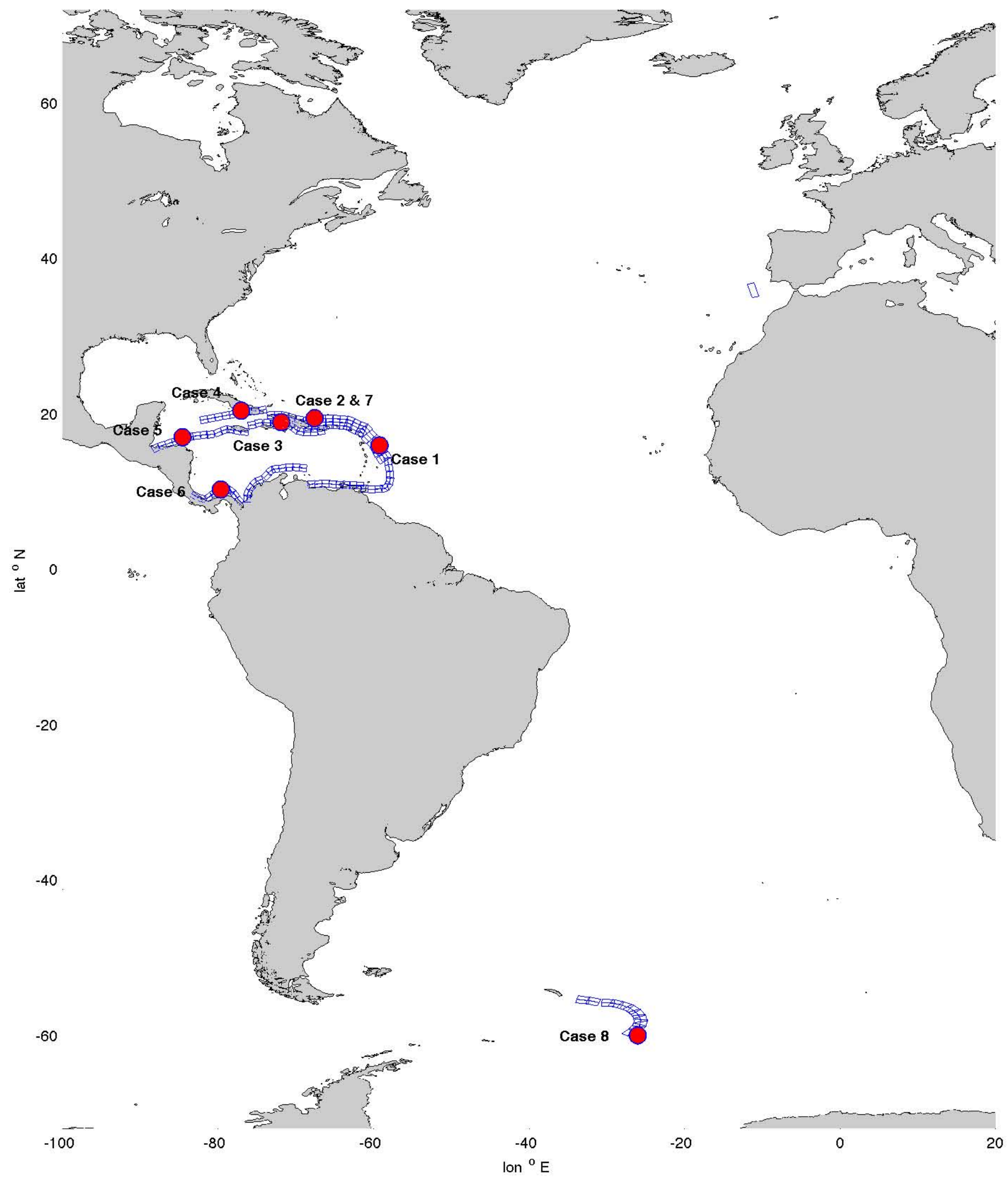


RIM Grids



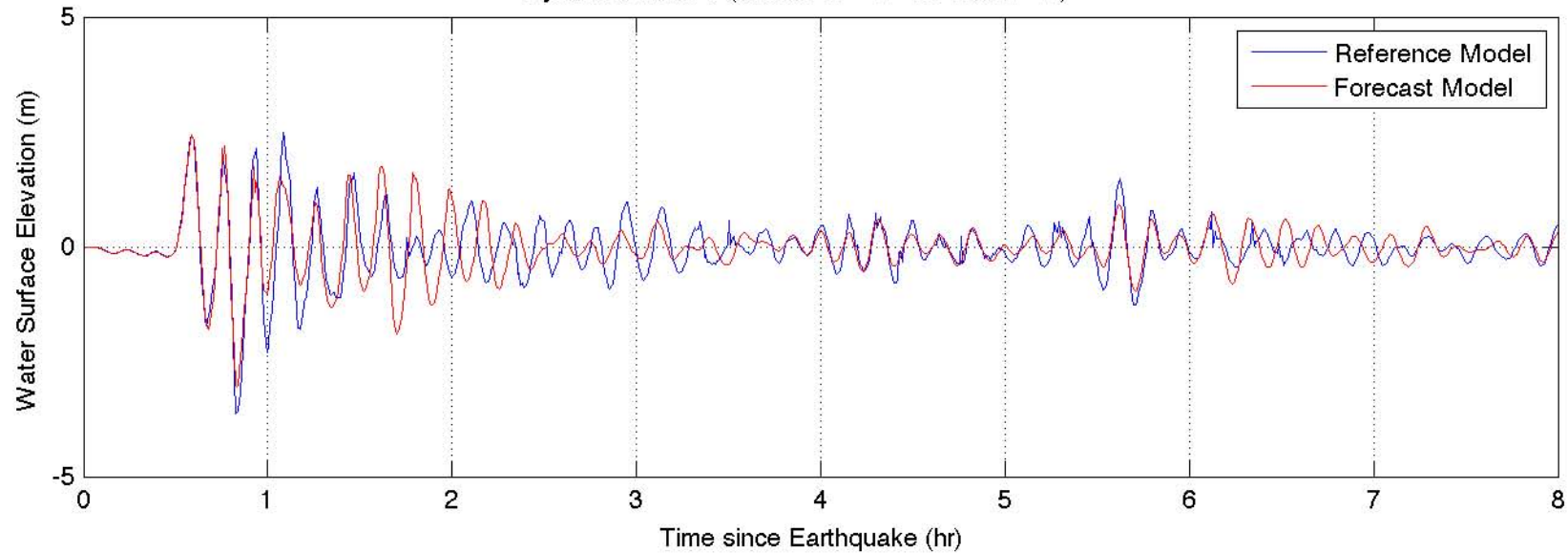
SIM Grids



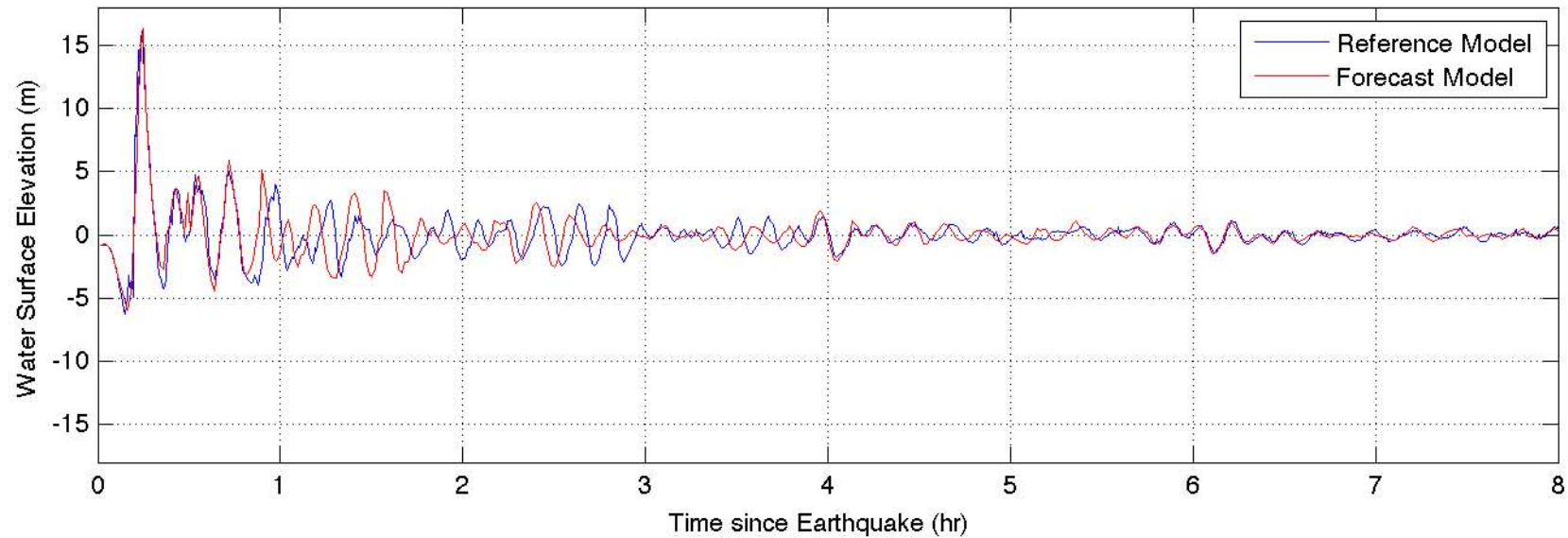




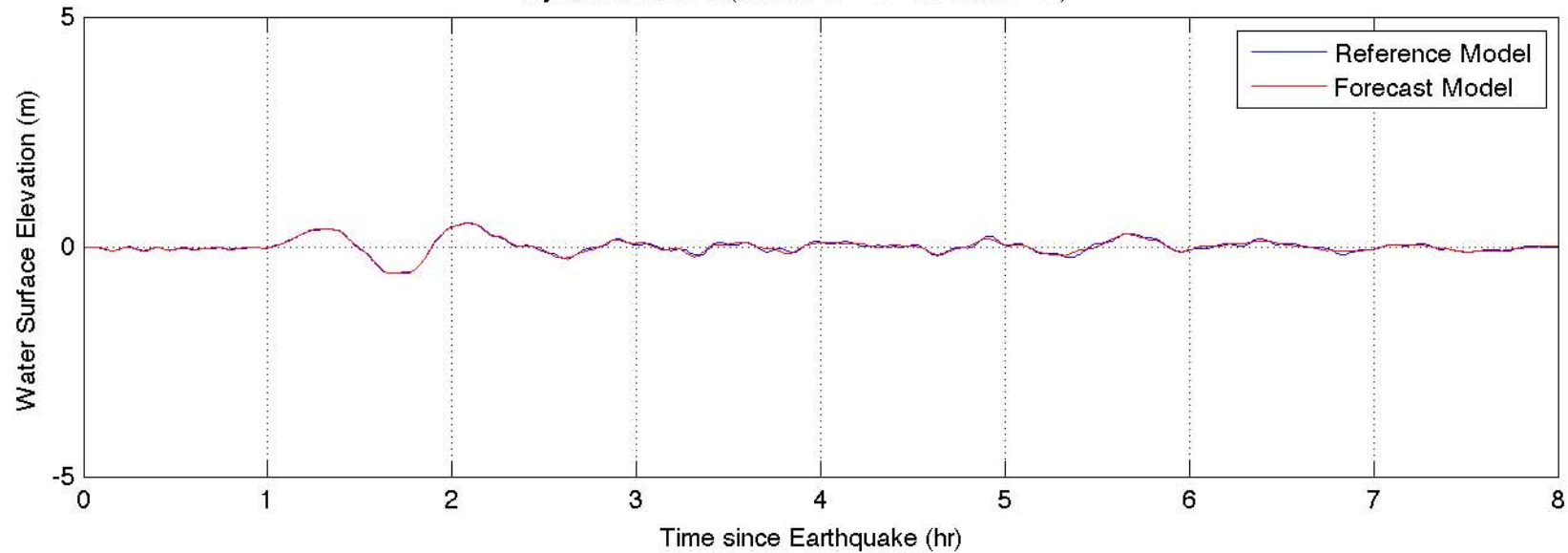
Synthetic Case 1 ( $66.70144^{\circ}$  W  $18.47912^{\circ}$  W)



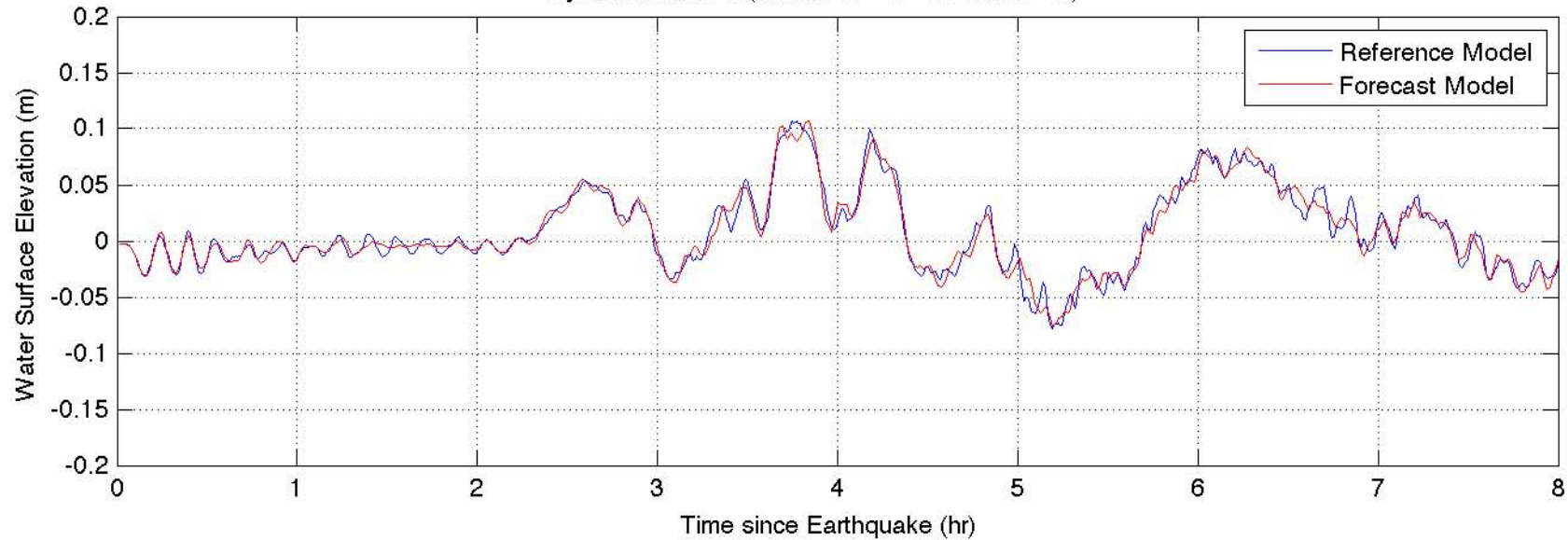
Synthetic Case 2 (66.70144° W 18.47912° W)



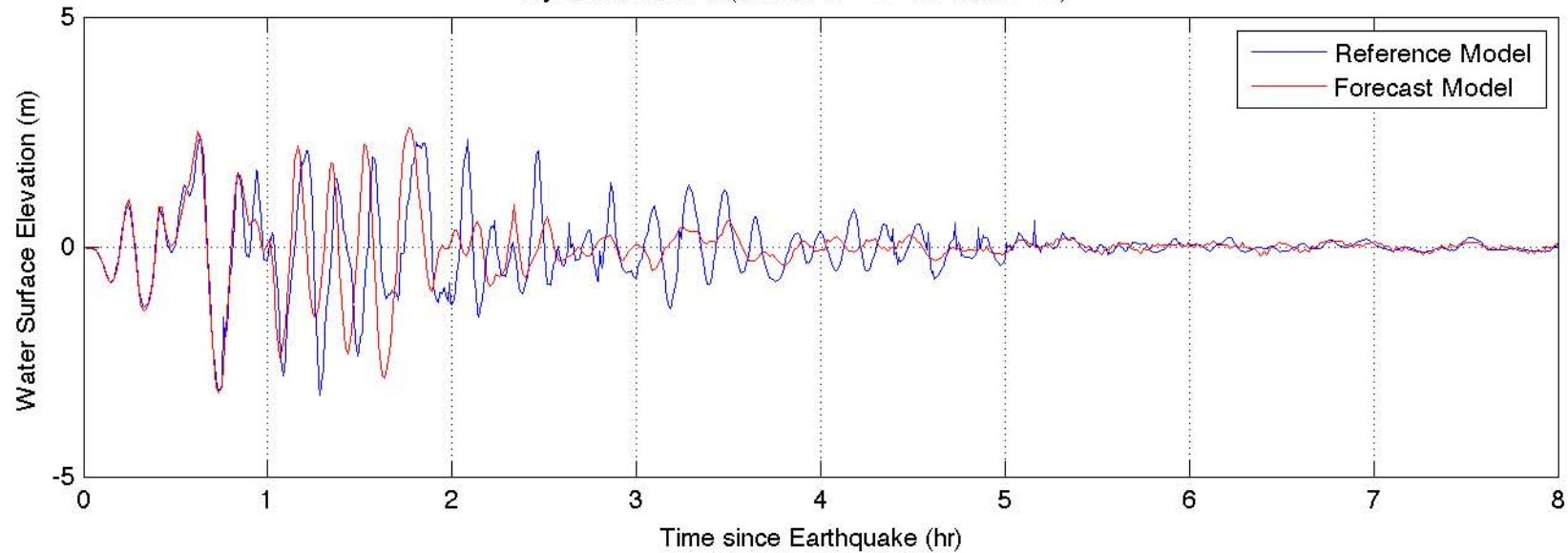
Synthetic Case 3 (66.70144° W 18.47912° W)



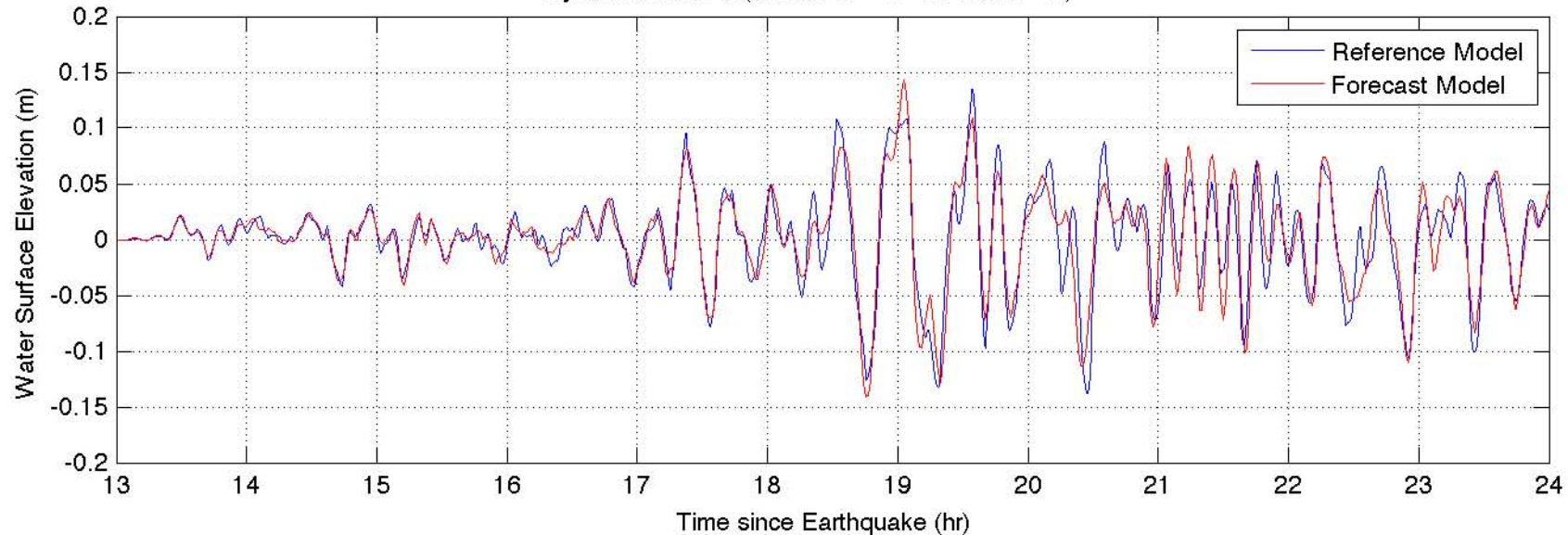
Synthetic Case 4 (66.70144° W 18.47912° W)



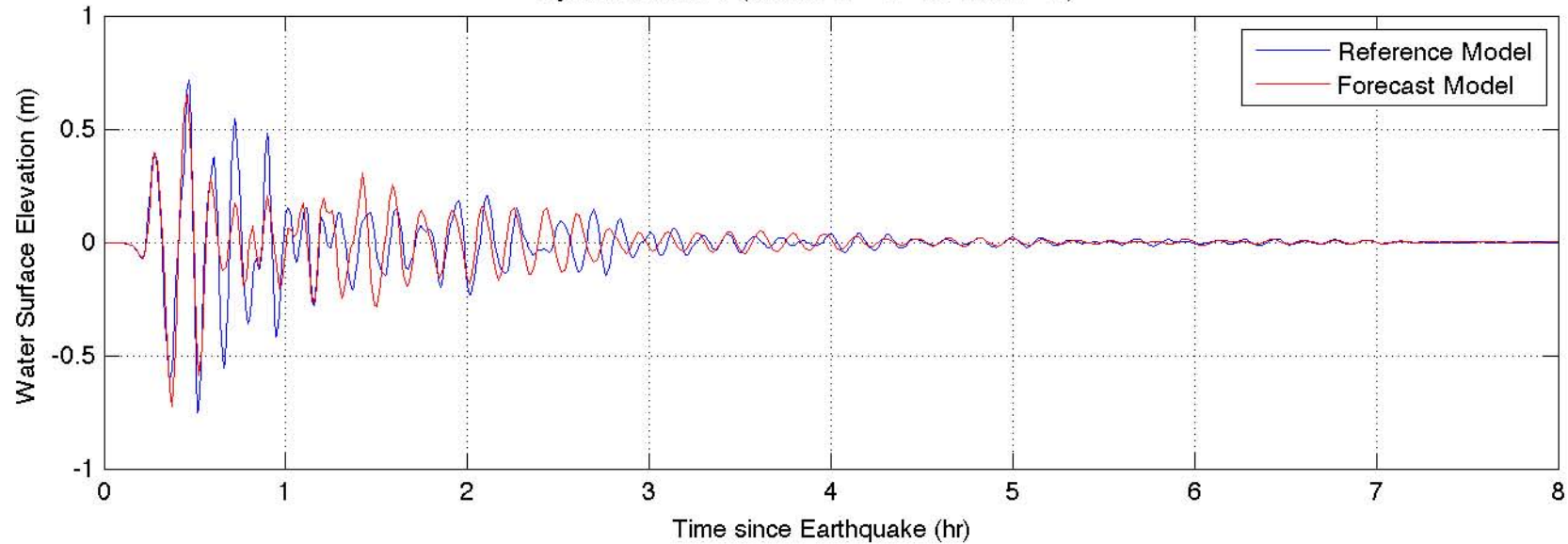
Synthetic Case 5 ( $66.70144^{\circ}$  W  $18.47912^{\circ}$  W)



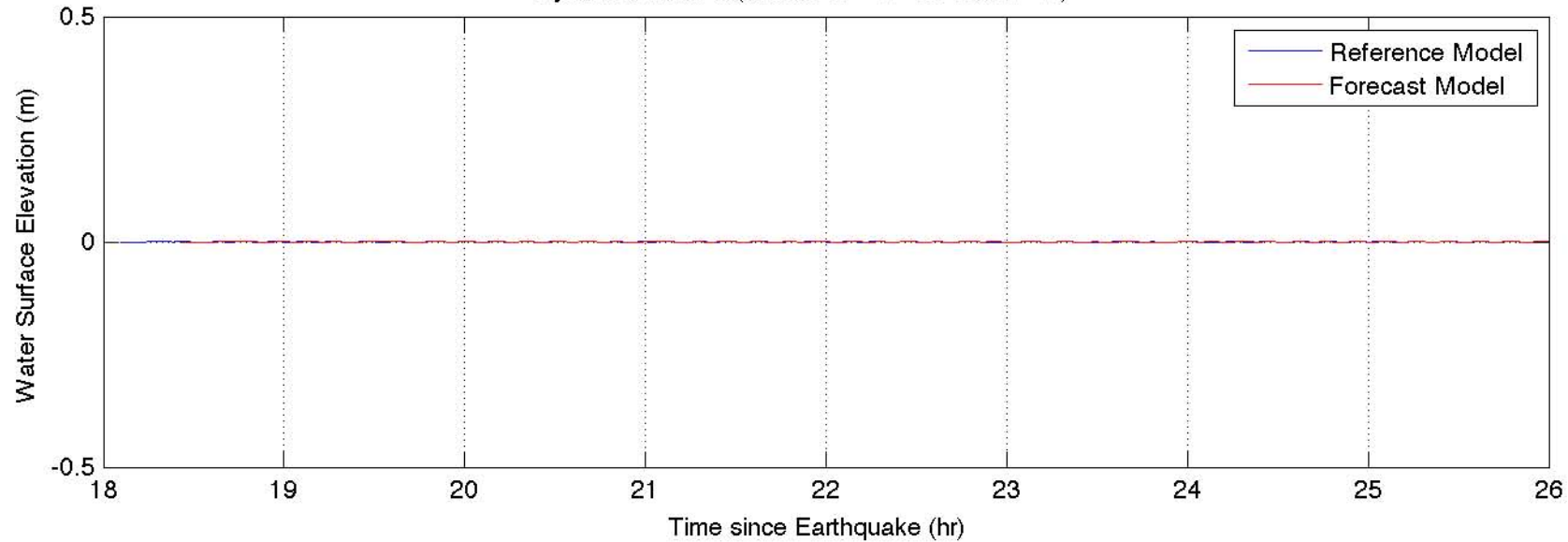
Synthetic Case 6 ( $66.70144^{\circ}$  W  $18.47912^{\circ}$  W)



Synthetic Case 7 ( $66.70144^{\circ}$  W  $18.47912^{\circ}$  W)

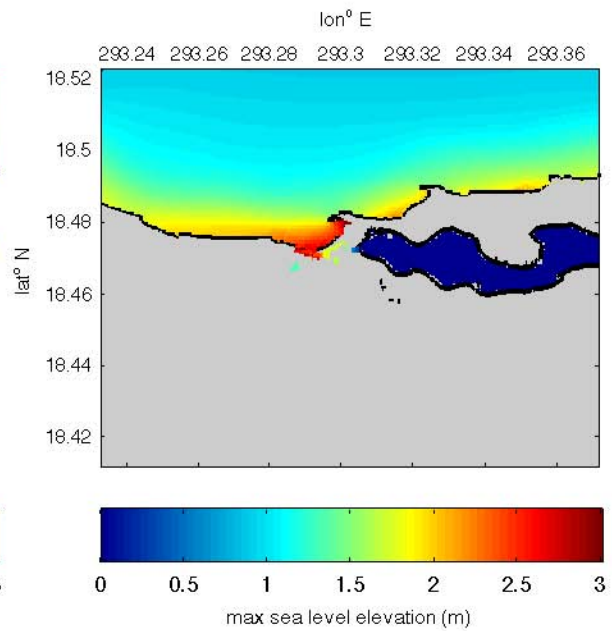
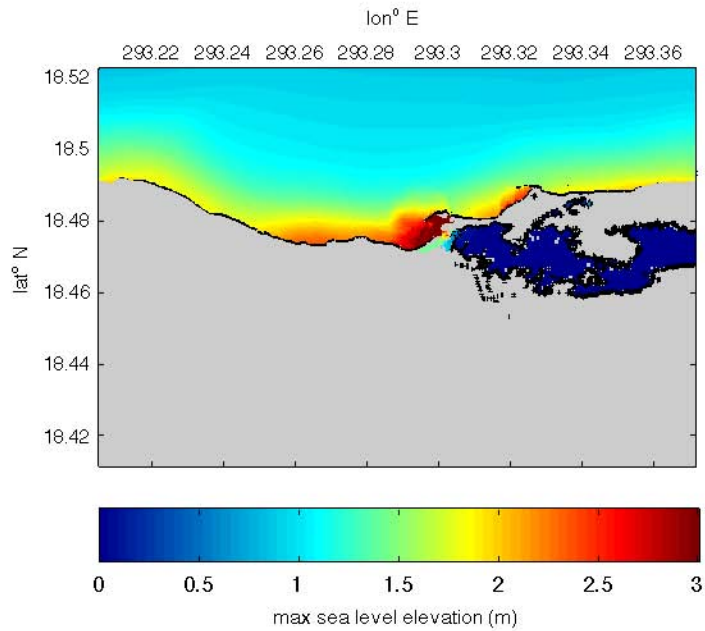


Synthetic Case 8 (66.70144° W 18.47912° W)

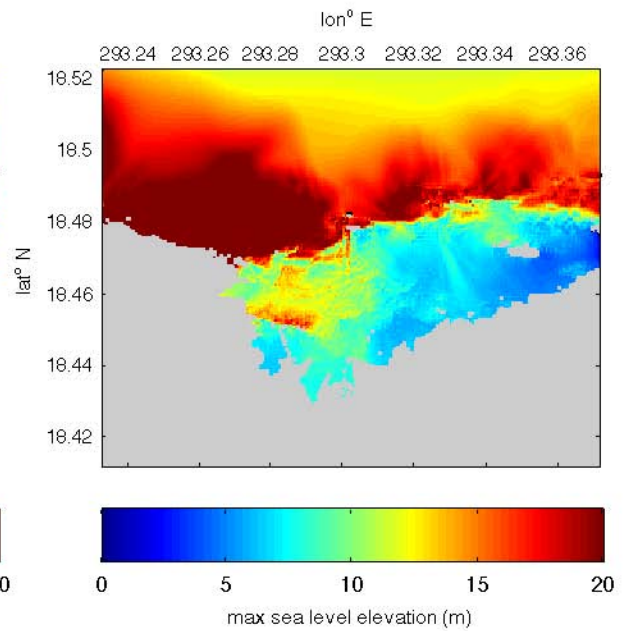
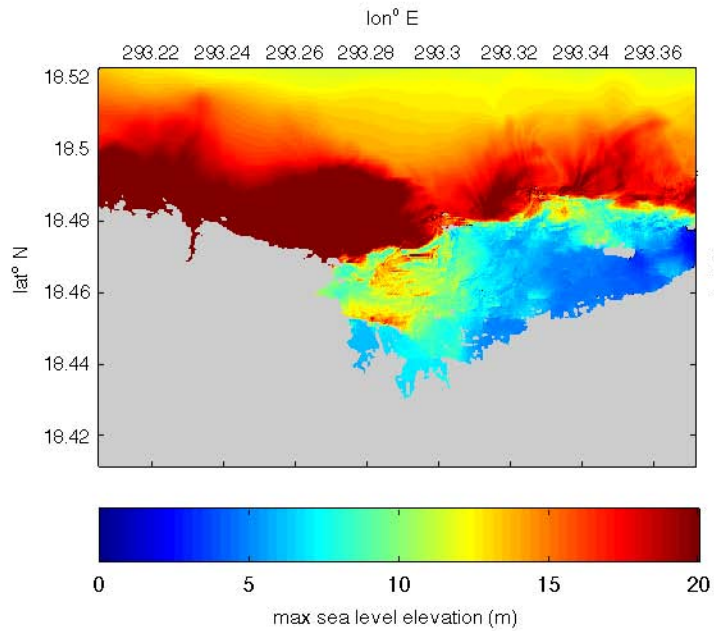




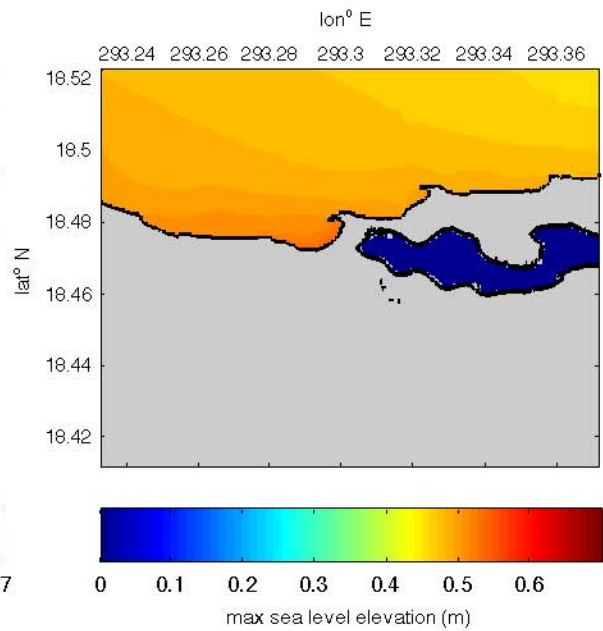
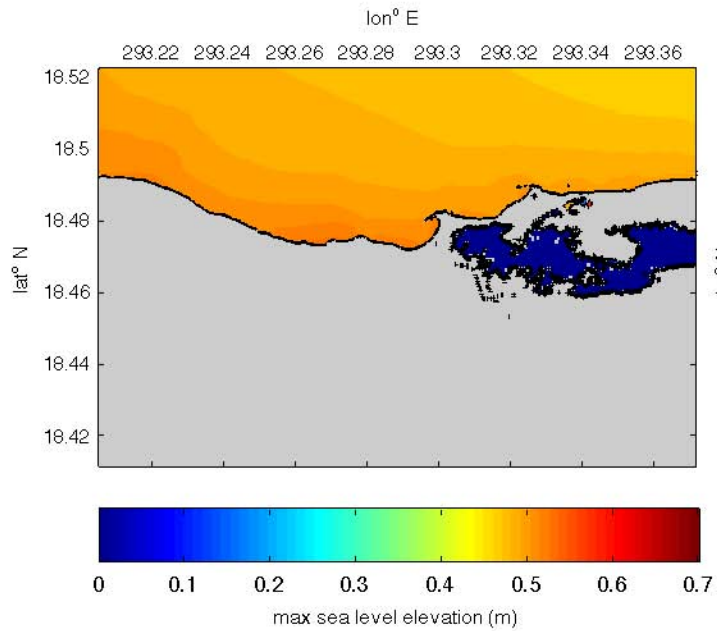
# Synthetic Case 1



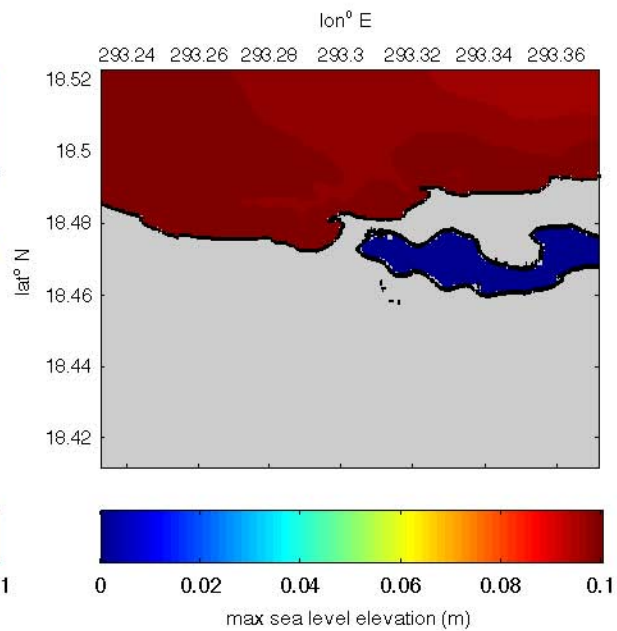
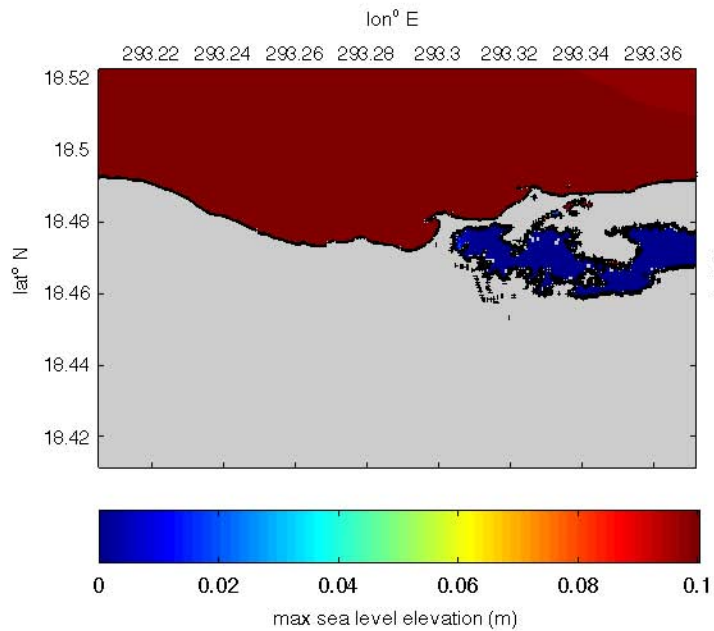
## Synthetic Case 2



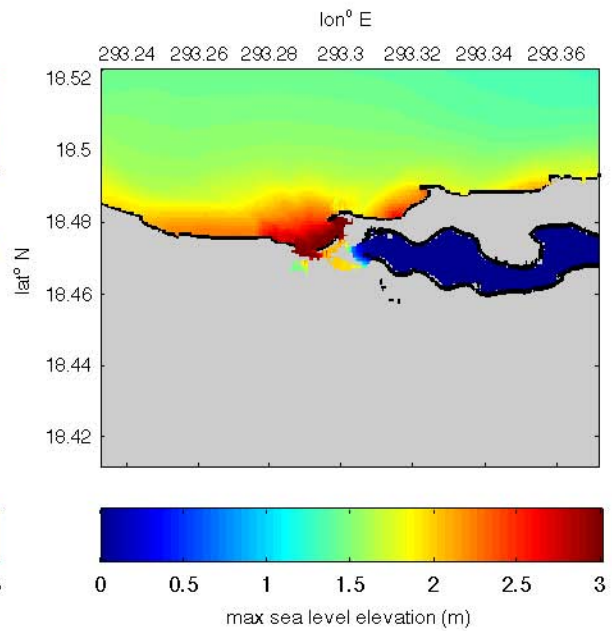
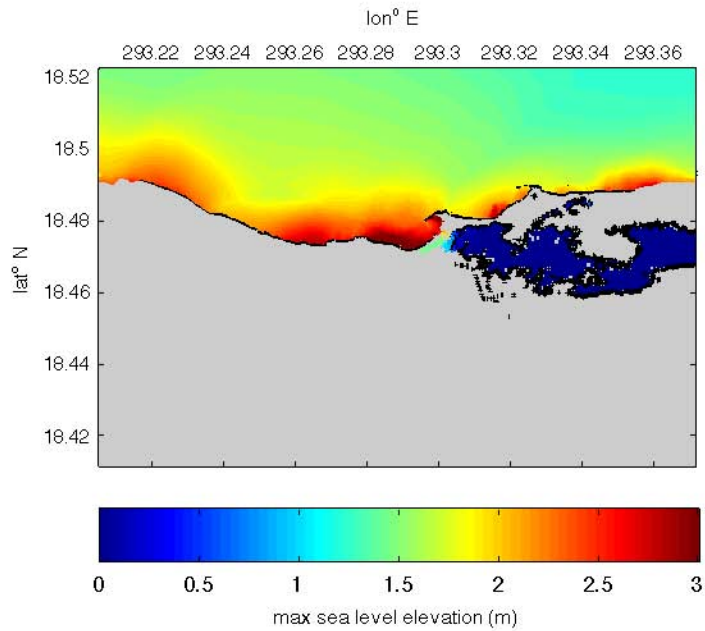
### Synthetic Case 3



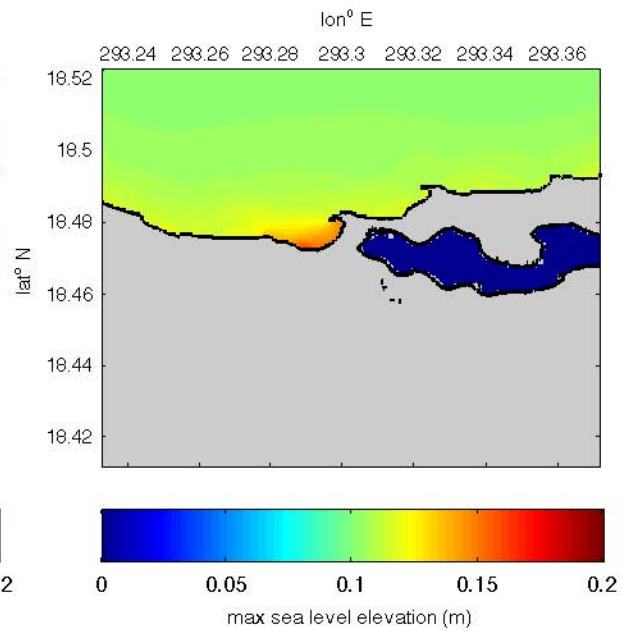
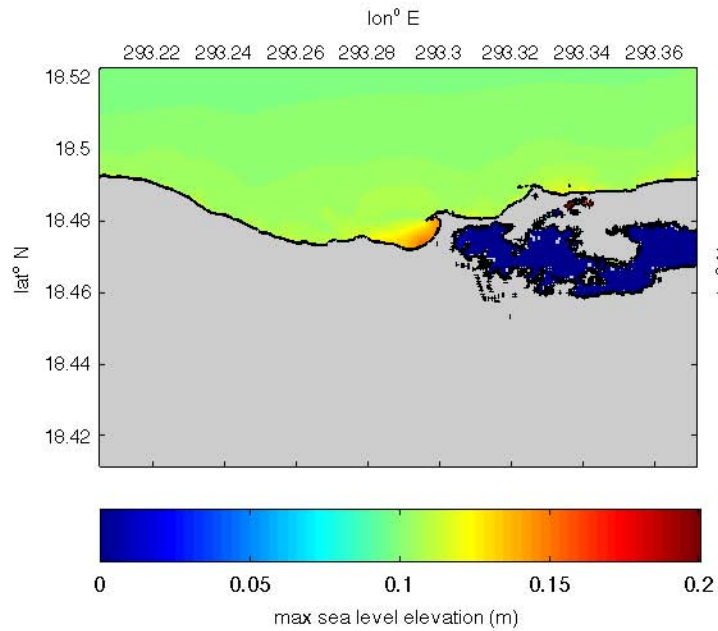
# Synthetic Case 4



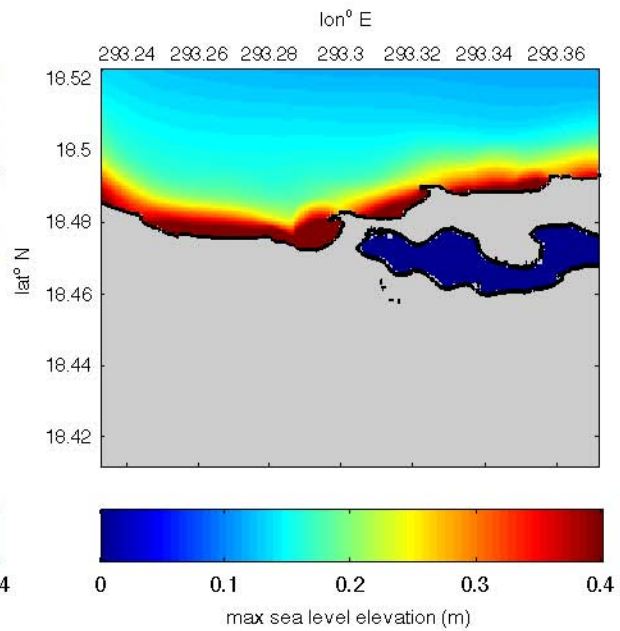
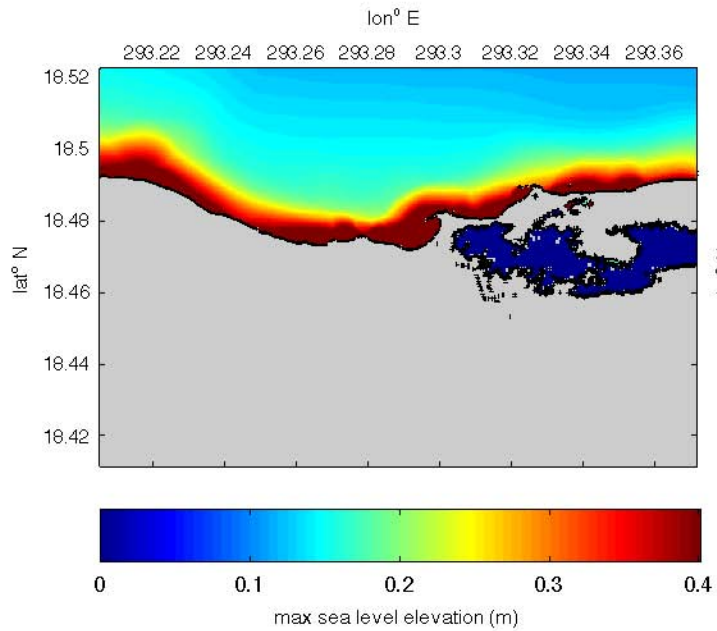
### Synthetic Case 5



# Synthetic Case 6



### Synthetic Case 8



### Synthetic Case 8

